vhp Is a Fibrinogen-Binding Protein Related to vWbp in *Staphylococcus aureus*

Sheila Thomas,ᵃ* Srishtee Arora,ᵃ Wen Liu,ᵃ Kelly Churion,ᵃ You Wu,ᵃ* Magnus Höökᵃ

ᵃCenter for Infectious and Inflammatory Diseases, Institute of Biosciences and Technology, Texas A&M University Health Science Center, Houston, Texas, USA

ABSTRACT *Staphylococcus aureus* can target a variety of tissues, causing life-threatening infections. The basis for this diversity stems from the microorganism's ability to spread in the vascular system throughout the body. To survive in blood, *S. aureus* coats itself with a fibrinogen (Fg)/fibrin shield. The protective shield is assembled by the coordinated actions of a number of Fg-binding bacterial proteins that manipulate the host's blood coagulation system. Several of the Fg binders appear redundant, sharing similar functional motifs. This observation led us to screen for the presence of novel proteins with significant amino acid identities to von Willebrand factor-binding protein (vWbp), a key component in the shield assembly machinery. One identified protein showed significant sequence identity with the C-terminal region of vWbp, and we consequently named it vWbp homologous protein (vhp). The *vhp* gene lies within a cluster of genes that encode other virulence factors in *S. aureus*. Although each isolate only contains one copy of the *vhp* gene, *S. aureus* has at least three distinct alleles, *vhpA, B,* and *C,* that are present in the core genome. All three vhp isoforms bind Fg with high affinity, targeting a site located in the D fragment of Fg. We further identified an ∼79 amino acid-long, conserved segment within the C-terminal region of vWbp that shares high sequence identities (54 to 67%) with the vhps and binds soluble Fg with high affinity. Further analysis of this conserved motif and the intact vhps revealed intriguing differences in the Fg binding behavior, perhaps suggesting that these proteins have similar but discrete functions in the shield assembly.

IMPORTANCE The life-threatening diseases caused by multidrug-resistant *Staphylococcus aureus* strains are a worldwide medical problem due to treatment limitations and the lack of an effective vaccine. The ability of *S. aureus* to coat itself with a protective fibrinogen (Fg)/fibrin shield allows the organism to survive in blood and to disseminate and cause invasive diseases. This process represents a promising target for novel antistaphylococcal treatment strategies but is incompletely understood. *S. aureus* expresses a number of Fg-binding proteins. Some of these proteins have apparently redundant functions. Proteins with similar functions often share a structural or functional motif with each other. In this study, we identified a protein homologous to the C-terminal of von Willebrand factor-binding protein (vWbp), a key contributor in the Fg shield assembly that also binds Fg. Further analysis allowed us to identify a common Fg-binding motif.

KEYWORDS *Staphylococcus aureus*, fibrinogen-binding proteins, vhp, vWbp homolog

The Gram-positive, opportunistic pathogen *Staphylococcus aureus* employs a multitude of molecular tactics to evade the host defense system. Assembling a protective fibrinogen (Fg)/fibrin shield around the bacterium appears to be particularly important for staphylococcal survival in blood (1–4). The Fg shield protects *S. aureus* from being engulfed by neutrophils and macrophages (1, 2). The resulting impaired bacterial clearance allows for *S. aureus* to propagate and disseminate into surrounding tissues, causing serious infections, such as sepsis, osteomyelitis, and endocarditis (5, 6).

Fg is an abundant (2 to 5 mg/ml) plasma glycoprotein that is expressed by hepatocytes in the liver (7–9). It consists of three pairs of nonidentical chains, Aα-, Bβ-, and γ-chains, that are linked by 29 disulfide bonds (8–11). A central domain known as the E region is adjoined to two lateral globular D regions via triple α-helical coil-coiled segments (9, 11). Discrete E and D fragments can be isolated after digestion of full-length Fg by plasmin (8–12).

Although Fg is best known for its role in blood coagulation, it also has an important role in the defense against pathogenic microbes. Upon tissue damage, synthesis of Fg is upregulated and is recruited to the site of injury, where it is converted to insoluble fibrin via the coagulation cascade (12, 13). Fibrin(ogen) adheres to the "platelet plug" to create the fibrin clot, curbing bleeding and impeding bacterial entry (3, 9, 11). In addition, Fg regulates bacterial clearance by neutrophils via its interaction with the leukocyte integrin receptor $\alpha_m\beta_2$, resulting in neutrophil adhesion to the endothelial surface and the release of signals for activating proinflammatory pathways (3, 14, 15). Given the importance of Fg in the defense against pathogenic microbes, it is no surprise that some bacteria attempt to counter this activity (3, 16–18).

S. aureus exploits the host's Fg and blood coagulation system in efforts to escape recognition and clearance by the host defense mechanisms. To this end, the microorganism expresses a number of Fg-binding proteins (3, 17–21). These include a group of structurally related cell wall-anchored proteins that belong to the microbial surface components recognizing adhesive matrix molecules (MSCRAMM) family (3, 17, 18) as well as a group of secreted proteins belonging to a protein family referred to as the secretable expanded repertoire adhesive molecules (SERAMs) (3, 6, 17, 19–21). Most of these Fg-binding proteins have been shown to act as virulence factors in different animal models of staphylococcal infections, and, in some cases, the Fg binding activities of these proteins have been shown to be required for their virulence activity (3, 4, 6, 19, 20, 22–24).

Many of the interactions between staphylococcal proteins and Fg have not been characterized in detail. Thus, there is an incomplete picture of how these proteins manipulate the host's Fg physiology. One of the key *S. aureus* Fg-binding proteins is von Willebrand factor-binding protein (vWbp), which can act as a coagulase but is also a high-affinity Fg binder (25–29). vWbp has been demonstrated to act as a virulence factor in a murine bacteremia model, although the specific feature or features of vWbp that are responsible for the protein's pathogenic activity remain unknown (1, 3, 25, 26). vWbp has at least two distinct Fg-binding sites located at its N- and C-terminal regions, respectively (27–29). The N-terminal region of vWbp exhibits a slightly higher affinity to immobilized Fg than its C-terminal half (reported apparent half-maximal binding concentrations [K_D] of 3.2 nM versus 38 nM, respectively [28]) and binds specifically to the N-terminal segment of the Fg β-chain (27). The C-terminal Fg-binding site has not been characterized. Although the C-terminal Fg-binding domain of vWbp is highly conserved among *S. aureus* isolates, the C-terminal region does not contain any of the known staphylococcal Fg-binding motifs (27, 30–32).

In the current study, we have identified a unique protein, vWbp homologous protein (vhp), that shows a high degree of amino acid sequence identity to a C-terminal domain in vWbp and binds Fg with high affinity. Although each isolate only contains one copy of the *vhp* gene, *S. aureus* can express at least three distinct isoforms, vhpA, B, and C. This Fg-binding activity of the three vhp isoforms is further characterized.

RESULTS

An *S. aureus* open reading frame encodes a unique protein homolog of the C-terminal section of vWbp. We initiated a search for proteins homologous to vWbp in *S. aureus* genomes by using BLAST with the full-length vWbp sequence. Our search identified three related hypothetical proteins that have a signal peptide at the N-terminal region and a relatively conserved segment at their C-terminal region that is shared with the C-terminal section of vWbp (40%, 48%, and 39% identity, respectively) (Fig. 1A and B) and were subsequently determined to be isoforms (see below). We called these proteins
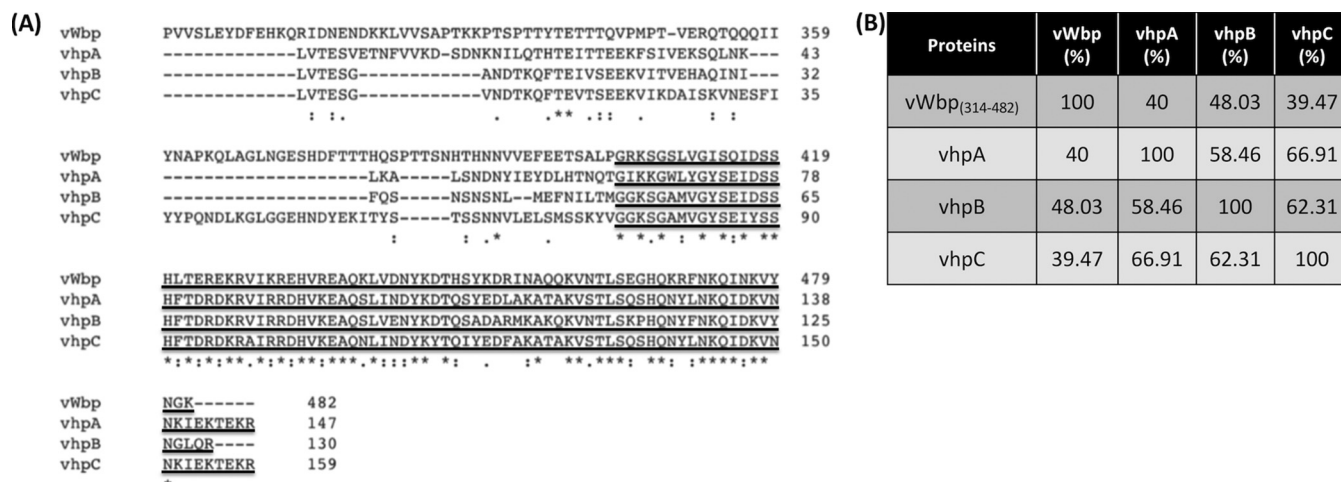
(A)

```
vWbp   PVVSLEYDFEHKQRIDNENDKKLVVSAPTKKPTSPTTYTETTTQVPMPT-VERQTQQQII  359
vhpA   -------------LVTESVETNFVVKD-SDNKNILQTHTEITTEEKFSIVEKSQLNK---   43
vhpB   -------------LVTESG---------ANDTKQFTEIVSEEKVITVEHAQINI---     32
vhpC   -------------LVTESG---------VNDTKQFTEVTSEEKVIKDAISKVNESFI     35
                    : :.               .    .** .::  .        : :

vWbp   YNAPKQLAGLNGESHDFTTTHQSPTTSNHTHNNVVEFEETSALPGRKSGSLVGISOIDSS  419
vhpA   --------------------LKA-----LSNDNYIEYDLHTNQTGIKKGWLYGYSEIDSS   78
vhpB   --------------------FQS-----NSNSNL--MEFNILTMGGKSGAMVGYSEIDSS   65
vhpC   YYPQNDLKGLGGEHNDYEKITYS-----TSSNNVLELSMSSKYVGGKSGAMVGYSEIYSS   90
                           :    :.*    .      * *.:  *  * *:* **

vWbp   HLTEREKRVIKREHVREAQKLVDNYKDTHSYKDRINAQQKVNTLSEGHQKRFNKQINKVY  479
vhpA   HFTDRDKRVIRRDHVKEAQSLINDYKDTQSYEDLAKATAKVSTLSQSHQNYLNKQIDKVN  138
vhpB   HFTDRDKRVIRRDHVKEAQSLVENYKDTQSADARMKAKQKVNTLSKPHQNYFNKQIDKVY  125
vhpC   HFTDRDKRAIRRDHVKEAQNLINDYKYTQIYEDFAKATAKVSTLSQSHQNYLNKQIDKVN  150
       *:*:*:**.*:*:**:***.*:::** *:  .   :*  **.***: **: :****:**

vWbp   NGK------  482
vhpA   NKIEKTEKR  147
vhpB   NGLQR----  130
vhpC   NKIEKTEKR  159
       *
```

(B)

Proteins	vWbp (%)	vhpA (%)	vhpB (%)	vhpC (%)
vWbp(314-482)	100	40	48.03	39.47
vhpA	40	100	58.46	66.91
vhpB	48.03	58.46	100	62.31
vhpC	39.47	66.91	62.31	100

FIG 1 vhp is homologous to vWbp-C$_{(386\ to\ 482)}$. (A) Clustal alignment of C-terminal vWbp, covering residues 242 to 482, and full-length vhpA, vhpB, and vhpC. Underlined residues indicate the conserved region. (B) Percent amino acid identity of vWbp$_{(314\ to\ 482)}$ *S. aureus* Newman (AAK52333.1), vhpA *S. aureus* N315 (BAB41978.1), vhpB *S. aureus* USA300_ FPR3757 (ABD21761.1), and vhpC *S. aureus* TCH60 (ADQ77850.1).

vWbp homologous protein A, B, or C (vhpA, vhpB, or vhpC, respectively). Full-length vhpA shares a 58% and 67% amino acid identity with that of full-length vhpB and vhpC, respectively (Fig. 1B). Between vhpB and vhpC there is a 62% sequence identity (Fig. 1B). However, the conserved C-terminal segment of vhpA (residues 63 to 147) shares a 70% identity with vhpB (residues 50 to 130) and an 87% identity with vhpC (residues 75 to 159) (Table S1 in the supplemental material). The percent identity of vhpB (residues 50 to 130) with vhpC (residues 75 to 159) is 70% (Table S1).

The vhpA, B, and C proteins are smaller than the 508 amino acid residue-long vWbp and are 173, 156, and 185 amino acid residues long, respectively (Fig. 1A and Fig. S1A and B). The vhps lack the two D domains found in the N terminus of staphylocoagulase (Coa) and vWbp, the characteristic first two N-terminal amino acids Val-Val of vWbp (33), and the Ile-Val of Coa (34) required for prothrombin activation. Therefore, vhps likely do not act as coagulases. The vhps also lack the 26 amino acid-long vWF-binding motif that is present in vWbp (Fig. 1 and Fig. S1A) (35).

The *vhp* gene is located in a gene cluster encoding known virulence factors. We located the gene encoding vhpA protein in the *S. aureus* strain N315 genome to a gene cluster that encodes known virulence factors. The gene cluster consists of *clfA*, *vWb*, *emp*, *vhp*, and *nuc* genes (Fig. 2) (35–37). This location is also observed for the *vhpB* gene from strain USA300_FPR3757 and the *vhpC* gene of strain TCH60 (Fig. 2). Thus, all three *vhp* genes are encoded in the same genetic location in different *S. aureus* strains, demonstrating that vhpA, B, and C proteins are isoforms of each other.

It is noteworthy that *clfA*, *vWb*, and *emp* genes encode Fg-binding proteins (21, 23, 27) that are known virulence factors, as demonstrated in murine *S. aureus* infection models (22, 23, 25, 38). Also, nuclease (Nuc) plays a role in virulence by degrading extracellular DNA traps released by neutrophils (37).

vhp is present in *S. aureus* as distinct isoform groups. We analyzed the genome sequences of 30 published clinical isolates with the goal to determine the genetic variation of *vhp* in relation to *vWb*. The isolates were obtained from different types of *S. aureus* infections from various geographical regions and represent a variety of sequence types (ST) (Table 1). Since the amino acid sequence differences between vhpA, B, and C were substantial, we referred to these sequences as prototypes of specific isotype groups (Table 1). We chose strain N315 as the prototype for vhpA, USA300_FPR3757 for vhpB, and TCH60 for vhpC, as these are also well-established clinical isolates. We assigned vhp isoforms to a particular group if they had an amino acid identity of 85 to 100% compared to the prototype of their respective isotype group (Table 1).
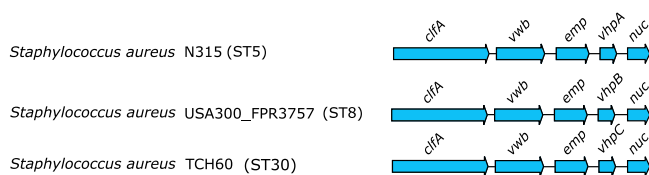
FIG 2 The *vhp* gene is located in a gene cluster encoding known virulence factors. A schematic representation of the organization of genes in the gene cluster. Blue arrowhead indicates a gene and the direction of translation. ST, sequence type.

A *vhp* gene is present in all isolates examined, and a majority (26 of 30) of the isolates examined belong to one of the identified isotype groups (vhpA, B, or C) (Table 1). Four of the 30 isolates, which included strains RF122, 08-02300, BB155, and 71193, do not fall into either group, suggesting the existence of additional isoforms besides vhpA, B, and C. The amino acid sequence from strain 71193 appears as a hybrid of vhpB and vhpC, in which the N-terminal region shows a relatively high similarity to the N-terminal region of vhpB, while its C-terminal region is nearly identical to the C-terminal segment of vhpC (Fig. S1A). Although the N-terminal amino acid sequence for both vhpAs of strains RF122 and 08–02300 are identical to vhpA, the C-terminal regions are identical to that of vhpB (Fig. S1A). Genome analysis of the strains revealed that only one *vhp* gene exists in each isolate.

We further examined a limited data set composed of 41 *S. aureus* ST5 isolates, 66 ST8 isolates, and 26 ST30 isolates. We found that all ST5 isolates contained vhpA, all ST30 isolates contained vhpC, and 66 of 68 ST8 isolates contained the vhpB isoform (Table S2).

We also analyzed the *vWb* gene to determine if a particular vWbp isoform is associated with any of the discrete vhp isoforms. Analysis of the 30 prototypic strains revealed at least 5 isoforms, which we termed as vWbpA, B, C, D, or E, respectively, based on an amino acid identity of 80 to 100% (Table 2; Table S3; Fig. S1B). The isolates also appear to carry only one *vwb* gene (Table 2) (35). We then examined whether there was a correlation between the vhp and vWbp isoforms (Table 2). It is noteworthy that the vWbpC isoforms are present in the strains that also harbor the vhpA isoforms, and the vWbpD isoforms are found in the strains that have vhpB (Table 2). However, vWbpA, B, and E isoforms do not appear to be present in isolates harboring specific vhp isoforms. Examining a larger set of isolates would likely reveal additional isoforms of both vhp and vWbp. Based on our results, it is possible that the two *S. aureus* proteins vhp and vWbp have evolved independently of each other.

Recombinant vhpA, B, and C bind Fg with high affinity. The C-terminal region of vWbp contains an Fg-binding site (27, 29). We therefore examined the Fg binding activity of the three major vhp isoforms using enzyme-linked immunosorbent assay (ELISA)-type binding assays (Fig. 3A and B) (27). We expressed and purified recombinant full-length vhpA, B, and C, each with a His_6-maltose-binding protein (MBP) tag fused to the N terminus (Fig. S2A). All three isoforms, when coated in microtiter wells, showed dose-dependent binding to soluble Fg with interactions that exhibited saturation kinetics. The calculated apparent K_D values (concentration required for half-maximum binding) were similar (29 nM, 41 nM, and 87 nM for vhpA, B, and C, respectively [Fig. 3A and Table 3]).

When tested for binding to Fg coated on the ELISA plates, the vhp isoforms also bound to immobilized Fg in a dose-dependent manner with apparent K_D values of 67 nM, 50 nM, and 100 nM, respectively (Fig. 3B and Table 3). As a negative control, a recombinant His_6-MBP fusion protein, purified by the same method used for purifying the recombinant vhps, showed no binding to soluble or immobilized Fg (Fig. S2B and C). Together, our data show that all three isoforms specifically bind to both soluble and immobilized Fg with similar high affinities.

The vhp isoforms bind to the Fg D fragment. To further characterize the interaction between Fg and vhp, we sought to identify the segment in Fg that binds to the

TABLE 1 Percent amino acid identity of vhp in 30 clinical S. aureus isolates

Strain name	ST[a]	vhp isoforms[b]	Protein ID[c]	CAI80 435.1[d]	ANI73 772.1[d]	AGO2 9166.1[d]	ADL2 2693.1[d]	CCG1 5434.1[d]	ADI97 346.1[d]	BAB9 4633.1[d]	AGU6 0934.1[d]	AMV8 4570.1[d]	BAB4 1978.1[d]	BAF7 7693.1[d]	ABR5 1687.1[d]
RF122	151	vhpA'	CAI80435.1	100[e]	96.45[e]	83.43[e]	85.8[e]	84.02[e]	86.39[e]	84.62[e]	86.39[e]	86.39[e]	86.98[e]	86.98[e]	86.98[e]
08-02300	7	vhpA'	ANI73772.1	96.45[e]	100[e]	83.43[e]	84.62[e]	84.02[e]	86.39[e]	84.62[e]	86.39[e]	86.39[e]	88.17[e]	88.17[e]	88.17[e]
CA-347	45	vhpA	AGO29166.1	83.43[e]	83.43[e]	100[e]	93.64[e]	93.06[e]	93.64[e]	94.8[e]	94.22[e]	94.22[e]	93.64[e]	93.64[e]	93.64[e]
JKD61 59	93	vhpA	ADL22693.1	85.8[e]	84.62[e]	93.64[e]	100[e]	92.49[e]	94.8[e]	95.38[e]	94.8[e]	94.8[e]	95.38[e]	95.38[e]	95.38[e]
HO 5096 0412	22	vhpA	CCG15434.1	84.02[e]	84.02[e]	93.06[e]	92.49[e]	100[e]	95.95[e]	94.8[e]	96.53[e]	96.53[e]	95.95[e]	95.95[e]	95.95[e]
ED133	133	vhpA	ADI97346.1	86.39[e]	86.39[e]	93.64[e]	94.8[e]	95.95[e]	100[e]	95.95[e]	97.69[e]	97.69[e]	98.27[e]	98.27[e]	98.27[e]
MW2	1	vhpA	BAB94633.1	86.39[e]	84.62[e]	94.8[e]	95.38[e]	94.8[e]	95.95[e]	100[e]	98.27[e]	98.27[e]	96.53[e]	96.53[e]	96.53[e]
CN1	72	vhpA	AGU60934.1	86.39[e]	86.39[e]	94.22[e]	94.8[e]	96.53[e]	97.69[e]	98.27[e]	100[e]	100[e]	98.27[e]	98.27[e]	98.27[e]
ST201 30943	25	vhpA	AMV84570.1	86.39[e]	86.39[e]	94.22[e]	94.8[e]	96.53[e]	97.69[e]	98.27[e]	100[e]	100[e]	98.27[e]	98.27[e]	98.27[e]
N315[f]	5	vhpA	BAB41978.1	86.98[e]	88.17[e]	93.64[e]	95.38[e]	95.95[e]	98.27[e]	96.53[e]	98.27[e]	98.27[e]	100[e]	100[e]	100[e]
Mu3	5	vhpA	BAF77693.1	86.98[e]	88.17[e]	93.64[e]	95.38[e]	95.95[e]	98.27[e]	96.53[e]	98.27[e]	98.27[e]	100[e]	100[e]	100[e]
JH1	105	vhpA	ABR51687.1	86.98[e]	88.17[e]	93.64[e]	95.38[e]	95.95[e]	98.27[e]	96.53[e]	98.27[e]	98.27[e]	100[e]	100[e]	100[e]
04-02981	225	vhpA	ADC36980.1	86.98[e]	88.17[e]	93.64[e]	95.38[e]	95.95[e]	98.27[e]	96.53[e]	98.27[e]	98.27[e]	100[e]	100[e]	100[e]
ST88	88	vhpA	AQD18902.1	86.98[e]	88.17[e]	93.64[e]	95.38[e]	95.95[e]	98.27[e]	96.53[e]	98.27[e]	98.27[e]	100[e]	100[e]	100[e]
ST228	228	vhpA	CCJ10585.1	85.8[e]	86.98[e]	92.49[e]	94.22[e]	94.8[e]	97.11[e]	95.38[e]	97.11[e]	97.11[e]	98.84[e]	98.84[e]	98.84[e]
MRSA 252	36	vhpC	CAG39854.1	56.96	55.7	70.37	69.14	69.75	69.14	69.14	69.14	69.14	68.52	68.52	68.52
TCH60[g]	30	vhpC	ADQ77850.1	56.96	55.7	70.37	69.14	69.75	69.14	69.14	69.14	69.14	68.52	68.52	68.52
ATCC 25923	243	vhpC	AIO20462.1	56.96	55.7	70.37	69.14	69.75	69.14	69.14	69.14	69.14	68.52	68.52	68.52
BB155	152	vhpC'	CRL33498.1	61.39	60.13	73.46	72.84	72.22	74.07	74.69	74.07	74.07	73.46	73.46	73.46
71193	398	vhpB'	AFH69102.1	60.9	59.62	70.62	70.62	74.38	73.75	72.5	73.75	73.75	73.12	73.12	73.12
NTCT 8325	8	vhpB	ABD29944.1	78.21	75.64	63.46	63.46	64.1	66.03	64.1	66.03	66.03	65.38	65.38	65.38
11819-97	80	vhpB	AEW64856.1	78.21	75.64	63.46	63.46	64.1	66.03	64.1	66.03	66.03	65.38	65.38	65.38
USA300_FP R3757[k]	8	vhpB	ABD21761.1	78.21	75.64	63.46	63.46	64.1	66.03	64.1	66.03	66.03	65.38	65.38	65.38
COL	250	vhpB	AAW36414.1	78.21	75.64	63.46	63.46	64.1	66.03	64.1	66.03	66.03	65.38	65.38	65.38
21282	254	vhpB	ELP41198.1	78.21	75.64	63.46	63.46	64.1	66.03	64.1	66.03	66.03	65.38	65.38	65.38
Newbould 305	115	vhpB	EJE56573.1	76.87	74.15	61.22	61.22	61.9	63.95	61.9	63.95	63.95	63.27	63.27	63.27
TW20	239	vhpB	CBI48744.1	78.21	75.64	63.46	63.46	64.1	66.03	64.1	66.03	66.03	65.38	65.38	65.38
M013	59	vhpB	AEV77849.1	77.56	75	62.82	62.82	63.46	65.38	63.46	65.38	65.38	64.74	64.74	64.74
MS4	338	vhpB	ALQ99050.1	77.56	75	62.82	62.82	63.46	65.38	63.46	65.38	65.38	64.74	64.74	64.74
6850	50	vhpB	AGU54604.1	67.86	66.07	66.07	66.96	65.18	67.86	66.96	67.86	67.86	66.96	66.96	66.96

[a]ST, sequence type.
[b]vhp isoforms indicate names of the isoforms.
[c]Protein ID is the accession number of the vhp isoforms.
[d]Percent identities of the vhp isoforms.
[e]vhpA isotype groups.
[f]Prototype for vhpA isotype group.
[g]Prototype for vhpC isotype group.
[h]vhpC isotype groups.
[i]Hybrid vhpB' isotype groups.
[j]vhpB isotype groups.
[k]Prototype for vhpB isotype group.

TABLE 1 (Continued)

ADC3 6980.1[d]	AQD1 8902.1[d]	CCJ10 585.1[d]	CAG3 9854.1[d]	ADQ7 7850.1[d]	AIO20 462.1[d]	CRL3 3498.1[d]	AFH6 9102.1[d]	ABD2 9944.1[d]	AEW6 4856.1[d]	ABD2 1761.1[d]	AAW3 6414.1[d]	ELP41 198.1[d]	EJE56 573.1[d]	CBI48 744.1[d]	AEV7 7849.1[d]	ALQ9 9050.1[d]	AGU5 4604.1[d]
86.98[e]	86.98[e]	85.8[e]	56.96	56.96	56.96	61.39	60.9	78.21	78.21	78.21	78.21	78.21	76.87	78.21	77.56	77.56	67.86
88.17[e]	88.17[e]	86.98[e]	55.7	55.7	55.7	60.13	59.62	75.64	75.64	75.64	75.64	75.64	74.15	75.64	75	75	66.07
93.64[e]	93.64[e]	92.49[e]	70.37	70.37	70.37	73.46	70.62	63.46	63.46	63.46	63.46	63.46	61.22	63.46	62.82	62.82	66.07
95.38[e]	95.38[e]	94.22[e]	69.14	69.14	69.14	72.84	70.62	63.46	63.46	63.46	63.46	63.46	61.22	63.46	62.82	62.82	66.96
95.95[e]	95.95[e]	94.8[e]	69.75	69.75	69.75	72.22	74.38	64.1	64.1	64.1	64.1	64.1	61.9	64.1	63.46	63.46	65.18
98.27[e]	98.27[e]	97.11[e]	69.14	69.14	69.14	74.07	73.75	66.03	66.03	66.03	66.03	66.03	63.95	66.03	65.38	65.38	67.86
96.53[e]	96.53[e]	95.38[e]	69.14	69.14	69.14	74.69	72.5	64.1	64.1	64.1	64.1	64.1	61.9	64.1	63.46	63.46	66.96
98.27[e]	98.27[e]	97.11[e]	69.14	69.14	69.14	74.07	73.75	66.03	66.03	66.03	66.03	66.03	63.95	66.03	65.38	65.38	67.86
98.27[e]	98.27[e]	97.11[e]	69.14	69.14	69.14	74.07	73.75	66.03	66.03	66.03	66.03	66.03	63.95	66.03	65.38	65.38	67.86
100[e]	100[e]	98.84[e]	68.52	68.52	68.52	73.46	73.12	65.38	65.38	65.38	65.38	65.38	63.27	65.38	64.74	64.74	66.96
100[e]	100[e]	98.84[e]	68.52	68.52	68.52	73.46	73.12	65.38	65.38	65.38	65.38	65.38	63.27	65.38	64.74	64.74	66.96
100[e]	100[e]	98.84[e]	68.52	68.52	68.52	73.46	73.12	65.38	65.38	65.38	65.38	65.38	63.27	65.38	64.74	64.74	66.96
100[e]	100[e]	98.84[e]	68.52	68.52	68.52	73.46	73.12	65.38	65.38	65.38	65.38	65.38	63.27	65.38	64.74	64.74	66.96
98.84[e]	98.84[e]	100[e]	67.9	67.9	67.9	72.22	71.88	64.1	64.1	64.1	64.1	64.1	61.9	64.1	63.46	63.46	65.18
68.52	68.52	67.9	100[h]	100[h]	100[h]	90.81[h]	83.12	66.67	66.67	66.67	66.67	66.67	64.63	66.67	64.74	64.74	68.75
68.52	68.52	67.9	100[h]	100[h]	100[h]	90.81[h]	83.12	66.67	66.67	66.67	66.67	66.67	64.63	66.67	64.74	64.74	68.75
68.52	68.52	67.9	100[h]	100[h]	100[h]	90.81[h]	83.12	66.67	66.67	66.67	66.67	66.67	64.63	66.67	64.74	64.74	68.75
73.46	73.46	72.22	90.81[h]	90.81[h]	90.81[h]	100[b]	77.5	71.79	71.79	71.79	71.79	71.79	70.07	71.79	69.87	69.87	75.89
73.12	73.12	71.88	83.12	83.12	83.12	77.5	100[b]	79.49[i]	79.49[i]	79.49[i]	79.49[i]	79.49[i]	78.91[i]	79.49[i]	78.21[i]	78.21[i]	85.71[i]
65.38	65.38	64.1	66.67	66.67	66.67	71.79	79.49[i]	100[i]	100[i]	100[i]	100[i]	100[i]	100[i]	100[i]	97.44[i]	97.44[i]	95.54[i]
65.38	65.38	64.1	66.67	66.67	66.67	71.79	79.49[i]	100[i]	100[i]	100[i]	100[i]	100[i]	100[i]	100[i]	97.44[i]	97.44[i]	95.54[i]
65.38	65.38	64.1	66.67	66.67	66.67	71.79	79.49[i]	100[i]	100[i]	100[i]	100[i]	100[i]	100[i]	100[i]	97.44[i]	97.44[i]	95.54[i]
65.38	65.38	64.1	66.67	66.67	66.67	71.79	79.49[i]	100[i]	100[i]	100[i]	100[i]	100[i]	100[i]	100[i]	97.44[i]	97.44[i]	95.54[i]
63.27	63.27	61.9	64.63	64.63	64.63	70.07	78.91[i]	100[i]	100[i]	100[i]	100[i]	100[i]	100[i]	100[i]	97.28[i]	97.28[i]	95.15[i]
65.38	65.38	64.1	66.67	66.67	66.67	71.79	79.49[i]	100[i]	100[i]	100[i]	100[i]	100[i]	100[i]	100[i]	97.44[i]	97.44[i]	95.54[i]
64.74	64.74	63.46	64.74	64.74	64.74	69.87	78.21[i]	97.44[i]	97.44[i]	97.44[i]	97.44[i]	97.44[i]	97.28[i]	97.44[i]	100[i]	100[i]	99.11[i]
64.74	64.74	63.46	64.74	64.74	64.74	69.87	78.21[i]	97.44[i]	97.44[i]	97.44[i]	97.44[i]	97.44[i]	97.28[i]	97.44[i]	100[i]	100[i]	99.11[i]
66.96	66.96	65.18	68.75	68.75	68.75	75.89	85.71[i]	95.54[i]	95.54[i]	95.54[i]	95.54[i]	95.54[i]	95.15[i]	95.54[i]	99.11[i]	99.11[i]	100[i]

TABLE 2 Percent amino acid identity of vWbp in clinical isolates

Strain name	ST[a]	vhp isoforms[b]	vWbp isoforms[c]	Protein ID (vWbp)[d]	AFH69 100.1[e]	AMV8 4568.1[e]	CRL3 3493.1[e]	ANI73 770.1[e]	CAI80 433.1[e]	EJE56 571.1[e]	CCG1 5432.1[e]	AEV7 7847.2[e]	ALQ9 9048.1[e]
RF122	151	vhpA'	vWbpB	CAI80433.1	79.16	82.16	82.93	84.37	100[f]	97.19[f]	92.59[f]	92.18[f]	92.18[f]
08-02300	7	vhpA'	vWbpA'	ANI73770.1	82.27[g]	84.06[g]	82.77[g]	100[g]	84.37	84.97	80.76	83.97	83.97
CA-347	45	vhpA	vWbpE	AGO29164.1	66.8	67.67	66.06	67.07	64.04	65.05	63.98	65.39	65.39
JKD6159	93	vhpA		ADL22691.1	67.27	67.74	65.92	67.34	68.15	67.55	67.07	68.69	68.69
HO 50960412	22	vhpA	vWbpB	CCG15432.1	79.16	79.76	80.92	80.76	92.59[f]	94.19[f]	100[f]	94.82[f]	94.82[f]
ED133	133	vhpA	vWbpC'	ADI97344.1	65.26	65.73	64.24	65.93	66.19	66.19	65.32	65.73	65.73
MW2	1	vhpA	trunc										
CN1	72	vhpA	trunc										
ST20130943	25	vhpA	vWbpA	AMV84568.1	93.82[g]	100[g]	94.39[g]	84.06[g]	82.16	83.37	79.76	80.36	80.36
N315[k]	5	vhpA											
Mu3	5	vhpA	vWbpC	BAF77691.1	66.4	67.68	66.8	68.48	66.73	67.14	65.86	65.66	65.66
JH1	105	vhpA	vWbpC	ABR51685.1	66.2	67.47	66.6	68.69	66.73	67.14	65.86	65.66	65.66
04-02981	225	vhpA	vWbpC	ADC36978.1	66.2	67.47	66.6	68.69	66.73	67.14	65.86	65.66	65.66
ST88	88	vhpA											
ST228	228	vhpA	vWbpC	CCJ10583.1	66.2	67.47	66.6	68.69	66.73	67.14	65.86	65.66	65.66
MRSA252	36	vhpC											
TCH60[l]	30	vhpC	vWbpE	ADQ77852.1	68.22	66.06	66.8	66.06	64.08	63.67	65.24	64.43	64.43
ATCC25923	243	vhpC	vWbpE	AIO20460.1	68.22	66.06	66.8	66.06	64.08	63.67	65.24	64.43	64.43
BB155	152	vhpC'	vWbpA	CRL33493.1	93.99[g]	94.39[g]	100[g]	82.77[g]	82.93	83.53	80.92	80.72	80.72
71193	398	vhpB'	vWbpA	AFH69100.1	100[g]	93.82[g]	93.99[g]	82.27[g]	79.16	80.36	79.16	78.96	78.96
NTCT8325	8	vhpB											
11819-97	80	vhpB	vWbpE	AEW64854.1	65.87	66.93	65.93	67.53	64.53	64.93	63.27	64.87	64.87
USA300_FPR3757[m]	8	vhpB	vWbpD	ABD20992.1	66	68.88	66.46	66.27	66.06	65.66	65.19	65.19	65.19
COL	250	vhpB	vWbpD	AAW36412.1	66	68.88	66.46	66.27	66.06	65.66	65.19	65.19	65.19
21282	254	vhpB	vWbpD	ELP41199.1	66	68.88	66.46	66.27	66.06	65.66	65.19	65.19	65.19
Newbould 305	115	vhpB	vWbpB	EJE56571.1	80.36	83.37	83.53	84.97	97.19[f]	100[f]	94.19[f]	92.18[f]	92.18[f]
TW20	239	vhpB	vWbpD	CBI48742.1	66	68.88	66.46	66.27	66.06	65.66	65.19	65.19	65.19
M013	59	vhpB	vWbpB	AEV77847.2	78.96	80.36	80.72	83.97	92.18[f]	92.18[f]	94.82[f]	100[f]	100[f]
MS4	338	vhpB	vWbpB	ALQ99048.1	78.96	80.36	80.72	83.97	92.18[f]	92.18[f]	94.82[f]	100[f]	100[f]
6850	50	vhpB	vWbpB	AGU54602.1	66.67	68.15	66.94	67.54	67.95	67.75	67.88	68.08	68.08

[a]ST, sequence type.
[b]Vhp isoforms indicate names of the isoforms.
[c]vWbp isoforms indicate names of the isoforms.
[d]Protein ID is the accession numbers of the vWbp isoforms.
[e]Percent identities of the vWbp isoforms.
[f]vWbpB isotype group.
[g]vWbpA isotype group.
[h]vWbpE isotype group.
[i]vWbpC isotype group.
[j]vWbpD isotype group.
[k]Prototype for vhpA isotype group.
[l]Prototype for vhpC isotype group.
[m]Prototype for vhpB isotype group.

TABLE 2 (Continued)

ADI97 344.1[e]	BAF7 7691.1[e]	ABR5 1685.1[e]	A DC3 6978.1[e]	CCJ10 583.1[e]	ABD2 0992.1[e]	AAW3 6412.1[e]	ELP41 199.1[e]	CBI48 742.1[e]	AGO2 9164.1[e]	ADQ7 7852.1[e]	AIO20 460.1[e]	AEW6 4854.1[e]	ADL2 2691.1[e]	AGU5 4602.1[e]
66.19	66.73	66.73	66.73	66.73	66.06	66.06	66.06	66.06	64.04	64.08	64.08	64.53	68.15	67.95
65.93	68.48	68.69	68.69	68.69	66.27	66.27	66.27	66.27	67.07	66.06	66.06	67.53	67.34	67.54
76.25	73.44	73.24	73.24	73.24	76.88	76.88	76.88	76.88	100[h]	91.42[h]	91.42[h]	92.14[h]	77.45	77.53
71.8	70.77	70.77	70.77	70.77	73.36	73.36	73.36	73.36	77.45	75.2	75.2	74.21	100	81.15
65.32	65.86	65.86	65.86	65.86	65.19	65.19	65.19	65.19	63.98	65.24	65.24	63.27	67.07	67.88
100	84.97[i]	84.97[i]	84.97[i]	84.97[i]	71.51	71.51	71.51	71.51	76.25	73.75	73.75	75	71.8	71.6
65.73	67.68	67.47	67.47	67.47	68.88	68.88	68.88	68.88	67.67	66.06	66.06	66.93	67.74	68.15
84.97	100[i]	99.8[i]	99.8[i]	99.8[i]	70.88	70.88	70.88	70.88	73.44	73.13	73.13	74.2	70.77	71.37
84.97	99.8[i]	100[i]	100[i]	100[i]	71.08	71.08	71.08	71.08	73.24	72.93	72.93	74	70.77	71.37
84.97	99.8[i]	100[i]	100[i]	100[i]	71.08	71.08	71.08	71.08	73.24	72.93	72.93	74	70.77	71.37
84.97	99.8[i]	100[i]	100[i]	100[i]	71.08	71.08	71.08	71.08	73.24	72.93	72.93	74	70.77	71.37
73.75	73.13	72.93	72.93	72.93	75.45	75.45	75.45	75.45	91.42[h]	100[h]	100[h]	92.43[h]	75.2	78.51
73.75	73.13	72.93	72.93	72.93	75.45	75.45	75.45	75.45	91.42[h]	100[h]	100[h]	92.43[h]	75.2	78.51
64.24	66.8	66.6	66.6	66.6	66.46	66.46	66.46	66.46	66.06	66.8	66.8	65.93	65.92	66.94
65.26	66.40	66.20	66.20	66.20	66.00	66.00	66.00	66.00	66.80	68.22	68.22	65.87	67.27	66.67
75	74.2	74	74	74	76.18	76.18	76.18	76.18	92.14[h]	92.43[h]	92.43[h]	100[h]	74.21	76.28
71.51	70.88	71.08	71.08	71.08	100[i]	100[i]	100[i]	100[i]	76.88	75.45	75.45	76.18	73.36	73.07
71.51	70.88	71.08	71.08	71.08	100[i]	100[i]	100[i]	100[i]	76.88	75.45	75.45	76.18	73.36	73.07
71.51	70.88	71.08	71.08	71.08	100[i]	100[i]	100[i]	100[i]	76.88	75.45	75.45	76.18	73.36	73.07
66.19	67.14	67.14	67.14	67.14	65.66	65.66	65.66	65.66	65.05	63.67	63.67	64.93	67.55	67.75
71.51	70.88	71.08	71.08	71.08	100[i]	100[i]	100[i]	100[i]	76.88	75.45	75.45	76.18	73.36	73.07
65.73	65.66	65.66	65.66	65.66	65.19	65.19	65.19	65.19	65.39	64.43	64.43	64.87	68.69	68.08
65.73	65.66	65.66	65.66	65.66	65.19	65.19	65.19	65.19	65.39	64.43	64.43	64.87	68.69	68.08
71.6	71.37	71.37	71.37	71.37	73.07	73.07	73.07	73.07	77.53	78.51	78.51	76.28	81.15	100

(A)

(B)
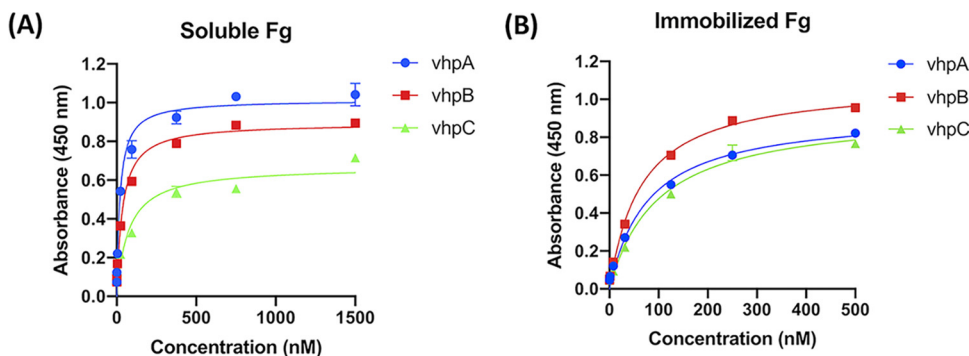
FIG 3 The vhp isoforms bind to immobilized and soluble Fg. (A) ELISA binding of soluble Fg to immobilized vhp isoforms (0.5 µg/well). (B) ELISA binding of vhp isoforms to immobilized Fg (0.5 µg/well). Error bars represent standard error of the mean (SEM). The graphs are representative of three independent experiments.

vhps (Fig. 4A to C). Fg was digested with the fibrinolytic enzyme plasmin to obtain two lateral globular D fragments (Fg-D) and a central E fragment (Fg-E) (7–13). We coated microtiter wells with full-length Fg, Fg-D, or Fg-E and examined the dose-dependent binding of the vhp isoforms to the isolated Fg fragments (Fig. 4A to C). The vhp isoforms bound to immobilized Fg-D in a dose-dependent manner that showed saturation kinetics and showed no binding to immobilized Fg-E. Binding of vhp isoforms to full-length Fg was used as a positive control (Table 3). The calculated apparent K_D values for vhpA, B, and C binding to the Fg-D fragment were 810 nM, 272 nM, and 244 nM, respectively (Table 3). The difference in apparent affinities of vhpA compared to vhpB or C could be due to the stability of the protein and the sequence variation noted among the proteins (Fig. 1A and Table 3). However, the apparent K_D values for the interaction between the Fg-D fragment and the vhp isoforms was around 10-fold higher than binding to full-length Fg, indicating that the Fg D fragment contains a partial binding site for the vhp proteins.

The Fg-binding motif of vWbp-C encompasses residues 386 to 482. We observed that amino acid residues ~386 to 482 of the C-terminal half of vWbp share high sequence identity with the vhp isoforms. Considering that both vWbp-C and vhp bind Fg, we speculated that amino acids 386 to 482 of vWbp might be responsible for Fg binding activity observed in the C-terminal half of the protein. We therefore expressed and purified the C-terminal region of vWbp, covering amino acid region 250 to 482 (vWbp-C) (27), and its two truncated versions, 250 to 386 (vWbp-C$_{[250\ to\ 386]}$) and 386 to 482 (vWbp-C$_{[386\ to\ 482]}$) (Fig. 5A and Fig. S2A). Using the ELISA-type binding assay, we determined that both vWbp-C and vWbp-C$_{(386\ to\ 482)}$ bind soluble Fg in a dose-dependent process that exhibited saturation kinetics (Fig. 5B; apparent K_D of 1.5 nM and 2.4 nM, respectively). Consistent with our earlier published data, vWbp-C showed weak binding to immobilized Fg (Fig. 5C and Table 3) (27). As expected, vWbp-C$_{(386\ to\ 482)}$ also showed little to no binding to immobilized Fg (Fig. 5C). Lastly, vWbp-C$_{(250\ to\ 386)}$ did not bind to either form of Fg under the experimental conditions used (Fig. S2D and E). His$_6$-MBP fusion protein was used as a negative control and showed no binding

TABLE 3 Half-maximal binding concentrations (K_D)

Protein	Soluble Fg (M)[a]	Immobilized Fg (M)[a]	Immobilized Fg-D (M)[a]	Immobilized Fg-E (M)[a]
vhpA[b]	$2.9 \times 10^{-8} \pm 1.5 \times 10^{-8}$	$6.7 \times 10^{-8} \pm 1.0 \times 10^{-8}$	$8.10 \times 10^{-7} \pm 4.3 \times 10^{-7}$	
vhpB[b]	$4.1 \times 10^{-8} \pm 2.2 \times 10^{-8}$	$5.0 \times 10^{-8} \pm 1.6 \times 10^{-8}$	$2.72 \times 10^{-7} \pm 6.9 \times 10^{-8}$	
vhpC[b]	$8.7 \times 10^{-8} \pm 1.2 \times 10^{-8}$	$1.0 \times 10^{-7} \pm 4.5 \times 10^{-8}$	$2.44 \times 10^{-7} \pm 7.5 \times 10^{-8}$	
vWbp-C	$1.5 \times 10^{-9} \pm 4.0 \times 10^{-10}$	ND[c]	ND	ND
vWbp-C$_{(386\ to\ 482)}$	$2.4 \times 10^{-9} \pm 6.3 \times 10^{-10}$	ND	ND	ND

[a]Averages of the half-maximal binding concentrations (M) and standard deviations.
[b]Full-length vhpA, B, and C.
[c]ND, not determined.
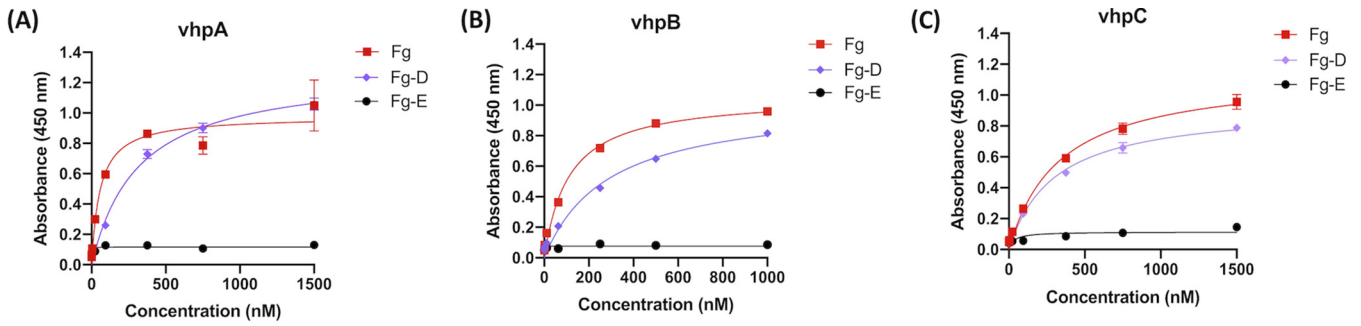
FIG 4 The vhp isoforms bind to the D fragment of Fg. ELISA binding of immobilized Fg fragments (0.5 μg/well) to vhp isoforms vhpA (A), vhpB (B), and vhpC (C); red, full-length Fg; purple, Fg D fragment; black, Fg E fragment. Error bars represent standard error of the mean (SEM). The graphs are representative of three independent experiments.

to both soluble and immobilized Fg (Fig. S2D and E). We concluded that the Fg-binding motif for the C-terminal half of vWbp is located at amino acid residues 386 to 482. Furthermore, this motif binds well to soluble Fg but not immobilized Fg, suggesting that vWbp binding to Fg requires a specific structural conformation of Fg that may not be available when Fg is immobilized in the microtiter well.

DISCUSSION

In this study, we identified a unique protein, vhp, which shows significant sequence identity to the Fg-binding C-terminal section of vWbp (Fig. 1A and B). *S. aureus* expresses multiple Fg-binding proteins, most of which are classified as MSCRAMMs (3, 17, 18) or SERAMs (3, 6, 17, 19–21). With the exception of vWbp, vhp does not share significant protein sequence identity or a notable motif with other Fg-binding proteins in *S. aureus*. Analysis of publicly available genomes of *S. aureus* clinical isolates revealed the presence of three distinct vhp isoforms A, B, and C. We identified Fg as a binding partner for all three isoforms. An initial characterization of this interaction showed that the vhps bind Fg with high affinity. The Fg D fragment, but not the E fragment, bound to the vhps, an observation that locates a vhp interactive site in Fg.
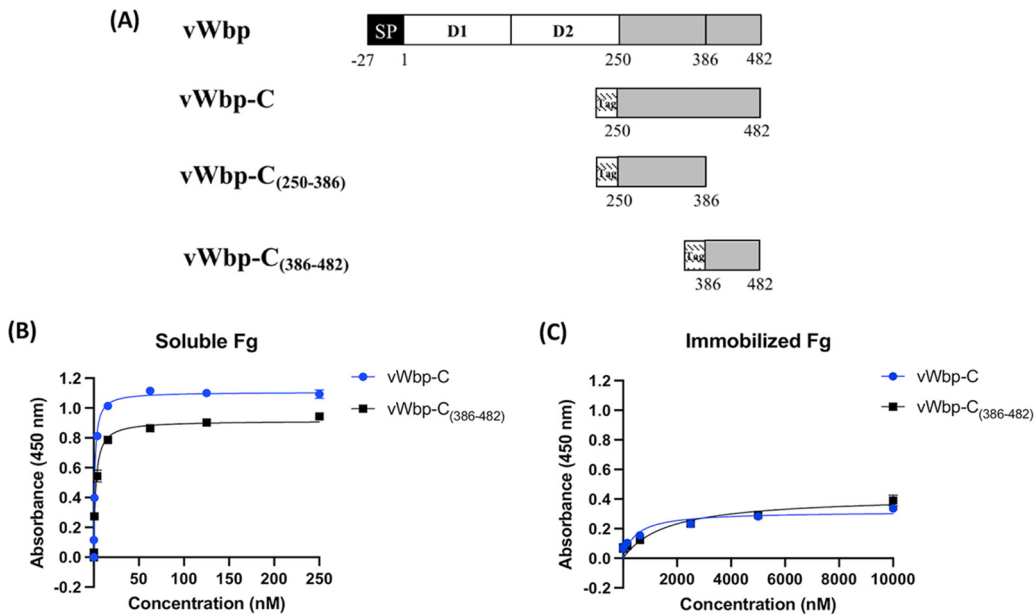
FIG 5 The C-terminal of vWbp harbors an Fg-binding site at residues 386 to 482. (A) Schematic overview of the vWbp constructs generated in this study. Gray represents the predicted unordered region; SP, signal peptide; D_1D_2, prothrombin-binding domain; Tag, N-terminal His$_6$-MBP tag. (B) ELISA binding of soluble Fg to immobilized vWbp constructs (0.5 μg/well). (C) ELISA binding of vWbp constructs to immobilized Fg (0.5 μg/well).

The sequence in the N-terminal half of the vhps shows a high degree of sequence variation between the isoforms. However, within each isoform group, the N-terminal region is conserved across different isolates (Fig. S1A in the supplemental material). This suggests that the N-terminal region of the isoforms might have different functions, perhaps interacting with different targets. The sequences of the C-terminal half of the vhps are conserved among isoforms of isolates and are highly homologous to residues 386 to 482 of vWbp. This vWbp segment was shown to contain a Fg-binding site. Since the prototypes of each vhp isoform behave similarly in their binding to Fg, it seems reasonable to conclude that Fg binding activity is located to the C-terminal region of all vhp isoforms.

Despite the similarities between vWbp and vhp, there are some significant differences in Fg binding between the two staphylococcal proteins. The apparent K_D of vWbp$_{(386\ to\ 482)}$ for binding to soluble Fg is about 10-fold lower than that shown for the binding of the vhp isoforms to Fg (Table 3). The vhp proteins bind the Fg D fragment with an apparent K_D of 10^{-7} M, whereas vWbp$_{(386\ to\ 482)}$ does not show any significant binding to the Fg D fragment under similar experimental conditions (Table 3) (data not shown). The vhps bind to Fg in the ELISA-type assay when Fg is adsorbed onto the microtiter plate and vhps are added in solution and when the assay is reversed such that the vhps are adsorbed on the plate and Fg is added in solution (Fig. 3). On the other hand, vWbp$_{(386\ to\ 482)}$ only binds to Fg when Fg is in solution. Soluble vWbp$_{(386\ to\ 482)}$ does not show significant binding to Fg adsorbed on the plate (Fig. 5). These observations could indicate that the vhps and vWbp$_{(386\ to\ 482)}$ bind Fg by different mechanisms. An alternative explanation is based on earlier studies by us and others, suggesting that the Fg binding of the C-terminal section of vWbp involves significant conformational arrangements in the two proteins (10, 27, 33, 39). This type of structural rearrangement could be inhibited when a protein is adsorbed in a microtiter plate in which protein flexibility may become restricted. To further define the Fg binding mechanism(s) in vhp and vWbp, the predicted conformational plasticity in the proteins needs to be examined.

vWbp along with Coa and extracellular fibrinogen-binding protein (Efb) appear to form a subfamily of functionally related secreted staphylococcal proteins where the members contribute to host defense evasion (3, 6, 20, 33). These multidomain molecules share homologous domains among each other (40). Both Coa and Efb have similar Fg-binding motifs that map to the intrinsically disordered regions of the proteins (3, 6). Coa and vWbp share a 30% amino acid identity at their N-terminal prothrombin-binding domains (30, 33, 34). They activate prothrombin by a similar mechanism, where the two N-terminal amino acid residues Ile^1-Val^2 and Val^1-Val^2, respectively, are inserted into the Ile^{16} pocket of prothrombin (33, 34). The now described vhp also fits into this family, as its C-terminal domain is highly homologous to the C-terminal Fg-binding section of vWbp. In addition, the extracellular complement-binding protein (Ecb) is related to Efb and shows 33% sequence identity to the C-terminal C3-binding domain of Efb, covering amino acid residues 65 to 136 of Efb (41, 42). Like *vWb* and *vhp*, the *ecb* and *efb* genes are located close to each other. Both *efb* and *ecb* genes are encoded in a mobile genetic element called IEC-2 (42).

The *vhp* gene is located within a gene cluster that includes genes coding for clumping factor A (ClfA), vWbp, extracellular matrix protein (Emp), and Nuc proteins (Fig. 2). The other proteins encoded in this cluster are identified as virulence factors that act by neutralizing the host defense system (1, 22, 25, 35, 37, 43). The location of *vhp* in the *S. aureus* genome raises a number of questions about the protein. Since all of the other proteins in this cluster are involved in evading host defenses, does vhp also participate in immune evasion? If yes, how does its interaction with Fg contribute to immune evasion? To what extent does vhp cooperate in its actions with the different proteins in this gene cluster? A possible functional cooperation among these proteins would require coordinated expression. As an example of this cooperation, ClfA and vWbp have been noted to interact with each other, resulting in enhanced adherence of

S. aureus to the endothelial vessel wall (44, 45). These and related questions will be topics for future studies.

MATERIALS AND METHODS

Bacterial strains and culture conditions. *Escherichia coli* strain Rosetta2(DE3) (Novagen) was used as the host for plasmid cloning and expression of His$_6$-MBP-tagged recombinant proteins. For the His$_6$-MBP-tagged fusion proteins, *E. coli* was grown on Terrific broth medium (Invitrogen) supplemented with kanamycin (50 μg/ml) and chloramphenicol (34 μg/ml).

Cloning of vhp and vWbp constructs. The *vhp* and *vwb* genes from *S. aureus* strain Newman were codon optimized and synthesized by Twist Biosciences (San Francisco, CA) as gene fragments. N-terminal His$_6$-MBP constructs vhpA/B/C/vWbp-C/vWbp-C$_{(386 \text{ to } 482)}$/or vWbp-C$_{(250 \text{ to } 386)}$ were generated using synthesized *vhp* or *vWb* gene fragments and were cloned into a pET28b (Agilent Technologies) plasmid. Fragments were digested with BamHI and Xhol using an In-Fusion cloning kit (TaKaRa Bio), resulting in the expression of N-terminal His$_6$-MBP constructs under the T7 *lac* promoter. Integrity of the resulting plasmid was confirmed by DNA sequencing.

Expression and purification of recombinant proteins. *E. coli* strains containing plasmids pET28b-vhpA/B/C/vWbp-C/vWbp-C$_{(386 \text{ to } 482)}$/or vWbp-C$_{(250 \text{ to } 386)}$ were grown overnight in Terrific broth medium containing chloramphenicol (34 μg/ml) and kanamycin (50 μg/ml) at 37°C. The overnight cultures were used to inoculate fresh Terrific broth medium containing kanamycin (50 μg/ml) and grown to an optical density at 600 nm (OD$_{600}$) of 0.8. After the culture was chilled to 4°C, recombinant expression was induced with 0.5 mM isopropyl 1-thio-β-D-galactopyranoside for 22 h at 22°C. Cells were harvested and resuspended in 50 mM Tris-HCl (pH 8.0) containing 300 mM NaCl, 20 mM imidazole, and 10% glycerol. The homogenous suspensions were centrifuged and lysed with two passes through an M-110p microfluidizer (Microfluidics International Corp.) at 20,000 lb/in^2 and then centrifuged at 30,000 $\times$ *g* for 1 h at 4°C. Supernatants were purified using a HisTrap HP 5-ml column (GE Healthcare), washed with phosphate-buffered saline (PBS; Gibco; pH 7.4) containing 35 mM imidazole, and eluted with 500 mM imidazole. Imidazole was removed by using a HiPrep 26/10 desalting column (GE Healthcare). Peak fractions were then loaded onto an MBPTrap HP 5-ml column (GE Healthcare) and eluted with PBS containing 10 mM maltose. All purifications were conducted on the ÄKTA pure system (GE Healthcare).

Gel permeation chromatography. Purified peak fractions from MBPTrap were further purified by loading onto a HiLoad 16/600 Superdex 200 pg column (GE Healthcare) preequilibrated with PBS. The fractions were pooled and concentrated using Amicon Ultra-15 centrifugal filters (10,000 nominal molecular weight limit [NMWL]) (Merck Millipore). Purification was conducted on the ÄKTA pure system. Protein purity was analyzed on SDS-PAGE gels stained with Coomassie blue R-250 (Sigma-Aldrich). Protein concentration was determined by a detergent-compatible protein assay with a Bio-Rad kit (Hercules, CA) using bovine serum albumin (BSA) as the standard.

Identification of vhp and isoforms. The vhp proteins were identified using BLAST. The amino acid sequence of vWbp, covering residues 250 to 482, was used to query bacterial genomes in the NCBI database. The presence of a vWbp-like open reading frame (ORF) was previously noted but not further explored (30). Analysis of the results was restricted to strains with finished genomes. Identified proteins were considered for analysis if they harbored a signal sequence, which was predicted by using SignalP-5.0 Server, and lacked both the prothrombin-binding and vWf-binding motifs of vWbp. Location of the *vhp* gene in the genome was determined by using the vhp amino acid sequence to search within the published genome as well as by identifying the proteins surrounding the sequence. A set of 33 *S. aureus* isolates representing multiple STs and with fully assembled genomes in publicly available databases (NCBI or Pathosystems Resource Integration Center [PATRIC]) were selected for further analysis. The vhp protein sequences were extracted from their respective genomes manually and aligned using Clustal Omega (46).

Fibrinogen. Human fibrinogen (FIB3, Enzyme Research Laboratories) was used in all experiments.

ELISA-type binding assay. Immulon 96-well microtiter plates (4HBX, Thermo Fisher Scientific) were used. Wells were coated overnight at 4°C with 100 μl of 5 μg/ml Fg/Fg-D/Fg-E or His$_6$-MBP-vWbp-C/vWbp-C$_{(386 \text{ to } 482)}$/vWbp-C$_{(250 \text{ to } 386)}$/vhpA/B/C (diluted in PBS). Plates were blocked with 3% BSA in Tris-buffered saline (TBS) (25 mM Tris, pH 7.4, 3 mM KCl, and 140 mM NaCl). For soluble Fg binding, diluted Fg (in 1% BSA, 0.05% Tween 20, and TBS) was added to coated wells of either the vWbp-C, vWbp-C$_{(386 \text{ to } 482)}$, vWbp-C$_{(250 \text{ to } 386)}$, or vhp proteins. For immobilized Fg binding, diluted recombinant vWbp-C, vWbp-C$_{(386 \text{ to } 482)}$, vWbp-C$_{(250 \text{ to } 386)}$, or vhp proteins (in 1% BSA, TBS, and 0.05% Tween 20) were added to the Fg/Fg-D/Fg-E-coated wells and incubated for 1 h at room temperature. Bound Fg was detected using horseradish peroxidase (HRP)-conjugated human Fg polyclonal antibodies (1:1,000 dilution; Rockland Immunochemicals, Inc.). HRP-conjugated anti-His polyclonal antibodies (1:3,000 dilution; R&D Systems) were used to detect bound recombinant proteins. Binding was quantified by the addition of substrate *o*-phenylenediamine dihydrochloride (Sigma-Aldrich), and the absorbance was measured at 450 nm using the ELISA microtiter plate reader (Biotek Cytation 5). A one-site binding equation was used to fit raw data, and apparent K_D values and goodness of fit (R^2) were obtained from GraphPad Prism software version 8.4.3. Apparent K_D values represent averages of three independent experiments.

Preparation of Fg fragments. Fg (Enzyme Research Laboratories) was digested with plasmin (10 μg/15 mg of Fg) (Enzyme Research Laboratories) in TBS containing 10 mM CaCl$_2$ for 4 h at 37°C as previously described (47) with modifications. Following plasmin digestion, Fg D fragment was obtained by column gel filtration on a Sephacryl S-200 (GE Healthcare) column with a molecular weight cutoff of 30 K, followed then by filtration in a column with a 50-K cutoff to remove plasmin. Purity of purified D fragments

was analyzed by SDS-PAGE and appeared as a single band with a molecular mass of 85 kDa. Human Fg E fragment (Fg-E) was purchased from Haematologic Technologies (HCI-0150E).

Accession numbers. vWbp from *S. aureus* Newman (AAK52333.1), vhpA from *S. aureus* N315 (BAB41978.1), vhpB from *S. aureus* USA300_ FPR3757 (ABD21761.1), and vhpC from *S. aureus* TCH60 (ADQ77850.1) are available from GenBank/EMBL under the accession numbers listed.

SUPPLEMENTAL MATERIAL

Supplemental material is available online only.

FIG S1, PDF file, 0.1 MB.

FIG S2, PDF file, 0.8 MB.

TABLE S1, PDF file, 0.1 MB.

TABLE S2, XLSX file, 0.01 MB.

TABLE S3, XLSX file, 0.04 MB.

REFERENCES

1. Guggenberger C, Wolz C, Morrissey JA, Heesemann J. 2012. Two distinct coagulase dependent barriers protect *Staphylococcus aureus* from neutrophils in a three dimensional in vitro model. PLoS Pathog 8:e1002434. https://doi.org/10.1371/journal.ppat.1002434.

2. Ko YP, Kuipers A, Freitag CM, Jongerius I, Medina E, van Rooijen WJ, Spaan AN, van Kessel KP, Höök M, Rooijakkers SH. 2013. Phagocytosis escape by a *Staphylococcus aureus* protein that connects complement and coagulation proteins at the bacterial surface. PLoS Pathog 9: e1003816. https://doi.org/10.1371/journal.ppat.1003816.

3. Ko YP, Flick MJ. 2016. Fibrinogen is at the interface of host defense and pathogen virulence in *Staphylococcus aureus* infection. Semin Thromb Hemost 42:408–421. https://doi.org/10.1055/s-0036-1579635.

4. Thomer L, Emolo C, Thammavongsa V, Kim HK, McAdow ME, Yu W, Kieffer M, Schneewind O, Missiakas D. 2016. Antibodies against a secreted product of *Staphylococcus aureus* trigger phagocytic killing. J Exp Med 213:293–301. https://doi.org/10.1084/jem.20150074.

5. Siddiqui AH, Koirala J. 2020. Methicillin-resistant *Staphylococcus aureus* (MRSA). Stat Pearls, Treasure Island, FL. https://www.ncbi.nlm.nih.gov/books/NBK482221/.

6. Ko YP, Kang M, Ganesh VK, Ravirajan D, Li B, Höök M. 2016. Coagulase and Efb of *Staphylococcus aureus* have a common fibrinogen binding motif. mBio 7:e01885-15. https://doi.org/10.1128/mBio.01885-15.

7. Mosesson MW. 2005. Fibrinogen and fibrin structure and functions. J Thromb Haemost 3:1894–1904. https://doi.org/10.1111/j.1538-7836.2005.01365.x.

8. Kattula S, Byrnes JR, Wolberg AS. 2017. Fibrinogen and fibrin in hemostasis and thrombosis. Arterioscler Thromb Vasc Biol 37:e13–e21. https://doi.org/10.1161/ATVBAHA.117.308564.

9. Weisel JW, Litvinov RI. 2017. Fibrin formation, structure and properties. Subcell Biochem 82:405–456. https://doi.org/10.1007/978-3-319-49674-0_13.

10. Kohler S, Schmid F, Settanni G. 2015. The internal dynamics of fibrinogen and its implications for coagulation and adsorption. PLoS Comput Biol 11:e1004346. https://doi.org/10.1371/journal.pcbi.1004346.

11. Wolberg AS, Campbell RA. 2008. Thrombin generation, fibrin clot formation and hemostasis. Transfus Apher Sci 38:15–23. https://doi.org/10.1016/j.transci.2007.12.005.

12. Gobel K, Eichler S, Wiendl H, Chavakis T, Kleinschnitz C, Meuth SG. 2018. The coagulation factors fibrinogen, thrombin, and factor XII in inflammatory disorders-a systematic review. Front Immunol 9:1731. https://doi.org/10.3389/fimmu.2018.01731.

13. Wolberg AS. 2007. Thrombin generation and fibrin clot structure. Blood Rev 21:131–142. https://doi.org/10.1016/j.blre.2006.11.001.

14. Flick MJ, Du X, Degen JL. 2004. Fibrin(ogen)-$\alpha_M\beta_2$ interactions regulate leukocyte function and innate immunity *in vivo*. Exp Biol Med (Maywood) 229:1105–1110. https://doi.org/10.1177/153537020422901104.

15. Flick MJ, Du X, Witte DP, Jirouskova M, Soloviev DA, Busuttil SJ, Plow EF, Degen JL. 2004. Leukocyte engagement of fibrin(ogen) via the integrin receptor $\alpha_M\beta_2$/Mac-1 is critical for host inflammatory response in vivo. J Clin Invest 113:1596–1606. https://doi.org/10.1172/JCI20741.

16. Buscetta M, Papasergi S, Firon A, Pietrocola G, Biondo C, Mancuso G, Midiri A, Romeo L, Teti G, Speziale P, Trieu-Cuot P, Beninati C. 2014. FbsC, a novel fibrinogen-binding protein, promotes *Streptococcus agalactiae*-host cell interactions. J Biol Chem 289:21003–21015. https://doi.org/10.1074/jbc.M114.553073.

17. Foster TJ, Höök M. 1998. Surface protein adhesins of *Staphylococcus aureus*. Trends Microbiol 6:484–488. https://doi.org/10.1016/s0966-842x(98)01400-0.

18. Foster TJ, Geoghegan JA, Ganesh VK, Höök M. 2014. Adhesion, invasion and evasion: the many functions of the surface proteins of *Staphylococcus aureus*. Nat Rev Microbiol 12:49–62. https://doi.org/10.1038/nrmicro3161.

19. McAdow M, Missiakas DM, Schneewind O. 2012. *Staphylococcus aureus* secretes coagulase and von Willebrand factor binding protein to modify the coagulation cascade and establish host infections. J Innate Immun 4:141–148. https://doi.org/10.1159/000333447.

20. Liesenborghs L, Verhamme P, Vanassche T. 2018. *Staphylococcus aureus*, master manipulator of the human hemostatic system. J Thromb Haemost 16:441–454. https://doi.org/10.1111/jth.13928.

21. Geraci J, Neubauer S, Pollath C, Hansen U, Rizzo F, Krafft C, Westermann M, Hussain M, Peters G, Pletz MW, Loffler B, Makarewicz O, Tuchscherr L. 2017. The *Staphylococcus aureus* extracellular matrix protein (Emp) has a fibrous structure and binds to different extracellular matrices. Sci Rep 7:13665. https://doi.org/10.1038/s41598-017-14168-4.

22. Cheng AG, Kim HK, Burts ML, Krausz T, Schneewind O, Missiakas DM. 2009. Genetic requirements for *Staphylococcus aureus* abscess formation and persistence in host tissues. FASEB J 23:3393–3404. https://doi.org/10.1096/fj.09-135467.

23. Flick MJ, Du X, Prasad JM, Raghu H, Palumbo JS, Smeds E, Höök M, Degen JL. 2013. Genetic elimination of the binding motif on fibrinogen for the *S. aureus* virulence factor ClfA improves host survival in septicemia. Blood 121:1783–1794. https://doi.org/10.1182/blood-2012-09-453894.

24. Scully IL, Timofeyeva Y, Keeney D, Matsuka YV, Severina E, McNeil LK, Nanra J, Hu G, Liberator PA, Jansen KU, Anderson AS. 2015. Demonstration of the preclinical correlate of protection for *Staphylococcus aureus* clumping factor A in a murine model of infection. Vaccine 33:5452–5457. https://doi.org/10.1016/j.vaccine.2015.08.029.

25. Cheng AG, McAdow M, Kim HK, Bae T, Missiakas DM, Schneewind O. 2010. Contribution of coagulases towards *Staphylococcus aureus* disease and protective immunity. PLoS Pathog 6:e1001036. https://doi.org/10.1371/journal.ppat.1001036.

26. Thomer L, Schneewind O, Missiakas D. 2016. Pathogenesis of *Staphylococcus aureus* bloodstream infections. Annu Rev Pathol 11:343–364. https://doi.org/10.1146/annurev-pathol-012615-044351.

27. Thomas S, Liu W, Arora S, Ganesh V, Ko YP, Höök M. 2019. The complex fibrinogen interactions of the *Staphylococcus aureus* coagulases. Front Cell Infect Microbiol 9:106. https://doi.org/10.3389/fcimb.2019.00106.

28. Thomer L, Schneewind O, Missiakas D. 2013. Multiple ligands of von Willebrand factor-binding protein (vWbp) promote *Staphylococcus aureus* clot formation in human plasma. J Biol Chem 288:28283–28292. https://doi.org/10.1074/jbc.M113.493122.

29. McAdow M, DeDent AC, Emolo C, Cheng AG, Kreiswirth BN, Missiakas DM, Schneewind O. 2012. Coagulases as determinants of protective immune responses against *Staphylococcus aureus*. Infect Immun 80:3389–3398. https://doi.org/10.1128/IAI.00562-12.

30. Bjerketorp J, Jacobsson K, Frykberg L. 2004. The von Willebrand factor-binding protein (vWbp) of *Staphylococcus aureus* is a coagulase. FEMS Microbiol Lett 234:309–314. https://doi.org/10.1016/j.femsle.2004.03.040.

31. Watanabe S, Ito T, Takeuchi F, Endo M, Okuno E, Hiramatsu K. 2005. Structural comparison of ten serotypes of staphylocoagulases in *Staphylococcus aureus*. J Bacteriol 187:3698–3707. https://doi.org/10.1128/JB.187.11.3698-3707.2005.

32. Viana D, Blanco J, Tormo-Mas MA, Selva L, Guinane CM, Baselga R, Corpa J, Lasa I, Novick RP, Fitzgerald JR, Penades JR. 2010. Adaptation of *Staphylococcus aureus* to ruminant and equine hosts involves SaPI-carried variants of von Willebrand factor-binding protein. Mol Microbiol 77:1583–1594. https://doi.org/10.1111/j.1365-2958.2010.07312.x.

33. Kroh HK, Panizzi P, Bock PE. 2009. Von Willebrand factor-binding protein is a hysteretic conformational activator of prothrombin. Proc Natl Acad Sci U S A 106:7786–7791. https://doi.org/10.1073/pnas.0811750106.

34. Panizzi P, Friedrich R, Fuentes-Prior P, Bode W, Bock PE. 2004. The staphylocoagulase family of zymogen activator and adhesion proteins. Cell Mol Life Sci 61:2793–2798. https://doi.org/10.1007/s00018-004-4285-7.

35. Bjerketorp J, Nilsson M, Ljungh A, Flock JI, Jacobsson K, Frykberg L. 2002. A novel von Willebrand factor binding protein expressed by *Staphylococcus aureus*. Microbiology (Reading) 148:2037–2044. https://doi.org/10.1099/00221287-148-7-2037.

36. Harraghy N, Homerova D, Herrmann M, Kormanec J. 2008. Mapping the transcription start points of the *Staphylococcus aureus* *eap*, *emp*, and *vwb* promoters reveals a conserved octanucleotide sequence that is essential for expression of these genes. J Bacteriol 190:447–451. https://doi.org/10.1128/JB.01174-07.

37. Thammavongsa V, Missiakas DM, Schneewind O. 2013. *Staphylococcus aureus* degrades neutrophil extracellular traps to promote immune cell death. Science 342:863–866. https://doi.org/10.1126/science.1242255.

38. Josefsson E, Higgins J, Foster TJ, Tarkowski A. 2008. Fibrinogen binding sites P336and Y338 of clumping factor A are crucial for *Staphylococcus aureus* virulence. PLoS One 3:e2206. https://doi.org/10.1371/journal.pone.0002206.

39. Kroh HK, Bock PE. 2012. Effect of zymogen domains and active site occupation on activation of prothrombin by von Willebrand factor-binding protein. J Biol Chem 287:39149–39157. https://doi.org/10.1074/jbc.M112.415562.

40. Patthy L. 1988. Detecting distant homologies of mosaic proteins. Analysis of the sequences of thrombomodulin, thrombospondin complement components C9, C8 alpha and C8 beta, vitronectin and plasma cell membrane glycoprotein PC-1. J Mol Biol 202:689–696. https://doi.org/10.1016/0022-2836(88)90550-5.

41. Hammel M, Sfyroera G, Ricklin D, Magotti P, Lambris JD, Geisbrecht BV. 2007. A structural basis for complement inhibition by *Staphylococcus aureus*. Nat Immunol 8:430–437. https://doi.org/10.1038/ni1450.

42. Jongerius I, Kohl J, Pandey MK, Ruyken M, van Kessel KP, van Strijp JA, Rooijakkers SH. 2007. Staphylococcal complement evasion by various convertase-blocking molecules. J Exp Med 204:2461–2471. https://doi.org/10.1084/jem.20070818.

43. McAdow M, Kim HK, Dedent AC, Hendrickx AP, Schneewind O, Missiakas DM. 2011. Preventing *Staphylococcus aureus* sepsis through the inhibition of its agglutination in blood. PLoS Pathog 7:e1002307. https://doi.org/10.1371/journal.ppat.1002307.

44. Claes J, Liesenborghs L, Peetermans M, Veloso TR, Missiakas D, Schneewind O, Mancini S, Entenza JM, Hoylaerts MF, Heying R, Verhamme P, Vanassche T. 2017. Clumping factor A, von Willebrand factor-binding protein and von Willebrand factor anchor *Staphylococcus aureus* to the vessel wall. J Thromb Haemost 15:1009–1019. https://doi.org/10.1111/jth.13653.

45. Claes J, Ditkowski B, Liesenborghs L, Veloso TR, Entenza JM, Moreillon P, Vanassche T, Verhamme P, Hoylaerts MF, Heying R. 2018. Assessment of the dual role of clumping factor A in *S. aureus* adhesion to endothelium in absence and presence of plasma. Thromb Haemost 118:1230–1241.

46. Sievers F, Wilm A, Dineen D, Gibson TJ, Karplus K, Li W, Lopez R, McWilliam H, Remmert M, Soding J, Thompson JD, Higgins DG. 2011. Fast, scalable generation of high-quality protein multiple sequence alignments using Clustal Omega. Mol Syst Biol 7:539. https://doi.org/10.1038/msb.2011.75.

47. Everse SJ, Pelletier H, Doolittle RF. 1995. Crystallization of fragment D from human fibrinogen. Protein Sci 4:1013–1016. https://doi.org/10.1002/pro.5560040523.